Research Article

41

INDONESIAN SCHOLAR SOCIETY

*Indones. J. Chem. Stud.*
2023, 2(2), 41–53
Available online at journal.solusiriset.com
e-ISSN: 2830-7658; p-ISSN: 2830-778X

Indonesian Journal of Chemical Studies

# Synthesis and Characterization of Isopropylidene Glycerol Acetate and Isopropylidene Glycerol Propanoate Compounds

Achmad Ridlo[1]*, Lutfia Choirunnisa[2], Fani Rahmawati[3], Aslan Irunsah[4], Bayu Ishartono[5]

[1]*Pharmacy Vocational Program, Poltekkes Kemenkes Surakarta, Klaten 57425, Indonesia*

[2]*Pharmacy and Food Analysis Program, Poltekkes Kemenkes Surakarta, Klaten 57425, Indonesia*

[3]*Department of Chemistry, The Republic of Indonesia Defense University, Bogor 16810, Indonesia*

[4]*Department of Biotechnology, Buton Institute of Marine Technology, Buton 93754, Indonesia*

[5]*Department of Chemistry, Universitas Gadjah Mada, Yogyakarta 55281, Indonesia*

Received: 19 Aug 2023; Revised: 07 Oct 2023; Accepted: 10 Oct 2023;
Published online: 23 Oct 2023; Published regularly: 31 Dec 2023

***Abstract—*** Isopropylidene Glycerol Acetate (IGA) and Isopropylidene Glycerol Propanoate (IGP) as ester compounds using acetic and propanoic acids have been synthesized, characterized, and studied for their antibacterial properties. The IGA was synthesized from ethyl acetate (EtOAc) and 1,2-O-isopropyliden glycerol (IPG) with a mole ratio of 1:8 through a transesterification reaction. Meanwhile, the IGP was synthesized using ethyl propanoate (EP) with the same ratio and method as IGA. All materials in this study were identified using FT-IR, GC-MS, $^{1}$H-NMR, and $^{13}$C-NMR. The characterization results indicated that the compounds of EP, IPG, IGA, and IGP had been successfully formed and identified. It was also revealed that the compounds of EP, IPG, IGA, and IGP were successfully synthesized with yields of 37.72, 27.78, 70.11, and 63.83%, respectively. The antibacterial activity test revealed that neither IGA nor IGP inhibited the growth of *Staphylococcus aureus* or *Escherichia coli* at concentrations of 62.5; 125; 250; 500; and 1000 ppm. Therefore, it was asserted that ester compounds synthesized with short-chain carboxylic acids, such as propanoic and acetic acids, lacked antibacterial properties.

***Keywords—*** *Isopropyliden glycerol; Isopropylidene glycerol acetate; Isopropylidene glycerol propanoate; Short chain carboxylic*

## 1. INTRODUCTION

The bacteria *Staphylococcus aureus* (*S. aureus*) and *Escherichia coli* (*E. coli*) represent gram-positive and gram-negative bacteria, respectively, which are responsible for diarrheic and acute digestive system issues in humans [1-2]. The presence of both bacteria in food products certainly poses a health hazard to humans. Therefore, it is important to prevent the presence of both bacteria. Several methods have been reported to inhibit the growth of these bacteria, including sonication with ultrasonic waves [3], [4], high-pressure processing [5], UV-irradiation [6], and hydrodynamic processing [1], as well as composite modification with the addition of chemicals [7]. However, some of these methods require high energy input and unaffordable preparation costs.

The use of chemicals in the form of ester compounds based on an esterification process followed by transesterification reactions is intriguing to be further studied and applied as antibacterial materials. The esterification reaction is the formation of ester compounds from carboxylic acid and alcohol [8]. The ester compounds produced from the esterification reaction use medium to long-chain carboxylic acids (C = 8, 10, 12, 14, and 16) and an alcohol compounds such as erythorbic acid resulted in an ester that possess the ability to inhibit the activity of gram-positive bacteria *Bacillus cereus* (*B. cereus*) but not gram-negative bacteria *E. coli* [9]. Other study also mention that ester compounds based on quinoline carboxamides exhibit high antibacterial activity against *Bacillus subtilis* (*B. subtilis*) and *S. aureus* [10].

Transesterification, as a continuation of the previous reaction in this study, is a substitution reaction of the organic alkyl group of an ester with alcohol compounds, catalyzed by acid or base catalysts, to produce new ester compounds [11]. Previous reports reported that the antibacterial material synthesized using transesterification reactions is produced also from the

***Corresponding author**.
Email address: ardridlo@gmail.com
DOI: 10.55749/ijcs.v2i2.30

use of medium and long-chain fatty acid compounds [12-13]. Throughout the literature review, no development of short-chain carboxylic acid-based monoglyceride derivative materials as antibacterial compounds has been reported. This study aim to synthesize and characterize Isopropylidene Glycerol Acetate (IGA) and Isopropylidene Glycerol Propanoate (IGP) as a candidate for antibacterial compunds precursor. The mechanism and characterization of the IGA and IGP has been comprehensively discuss in this paper.

## 2. EXPERIMENTAL SECTION

### 2.1. Materials

The chemicals used in this study were supplied from Merck which were directly used without further purification, including ethyl acetate (EtOAc) (CAS 141-78-6), propionic acid (PA) (CAS 79-09-4), glycerol (Gly) (CAS 56-81-5), sulfuric acid ($H_2SO_4$) (CAS 7664-93-9), absolute ethanol (CAS 64-17-5), acetone (CAS 67-64-1), n-hexane (CAS 110-54-3), sodium carbonate ($Na_2CO_3$) (CAS 497-19-8), calcium chloride ($CaCl_2$) (CAS 10043-52-4), pH universal indicator, para-toluene sulphonic acid (*p*TsOH) (CAS 6192-52-5), silica gel (CAS 7631-86-9), anhydrous sodium sulfate ($Na_2SO_4$) (CAS 7757-82-6), and thin layer chromatography (TLC) sheets with specification of silica gel 60 $F_{254}$ (20x20 cm).

The materials used for the antibacterial test were also produced by Merck, included nutrient broth (NB 105443), dimethyl sulfoxide (DMSO) (CAS 67-68-5), amoxicillin (CAS 26787-78-0), buffer solution, and agar. Distilled water, label paper, aluminium foil were supplied by CV. ARD Pratama as a local chemical store in Yogyakarta, Indonesia. The bacteria used were *S. aureus* and *E. coli* obtained from the Microbiology Laboratory of Faculty of Veterinary Medicine, Universitas Gadjah Mada, Yogyakarta, Indonesia.

### 2.2. Instrumentations

The equipment used in this study was a set of glassware, reflux apparatus, simple distillation apparatus, rotary evaporator, hotplate with magnetic stirrer IKA® C-MAG HS7, electronic weighing apparatus Libror EB- 330 Shimadzu, chamber, 254 and 366 nm UV lamps, and antibacterial kit tests. Functional group analysis was conducted by Fourier Transform Infrared spectrophotometer (FT-IR) Shimadzu Prestige 21. Chemical structure analysis was performed by Gas Chromatography-Mass Spectrometer (GC-MS) AGILENT GC type 5973 Shimadzu QP 2010S, and $^1$H-NMR and $^{13}$C-NMR 500 MHz JEOL JNM ECA 500 using TMS internal standard and chloroform solvent ($^1$H-NMR 7.26 ppm and $^{13}$C-NMR 77.2 ppm).

### 2.3. Esterification of Ethyl Propanoate (EP)

Propanoic Acid (PA) (0.25 mol) was reacted with ethanol (0.25 mol) and 4 mL $H_2SO_4$ catalyst and refluxed for 2 h at 80 °C. The reflux product was neutralized with 28.30 mmol $Na_2CO_3$ in 15 mL distilled water and extracted with 27.02 mmol $CaCl_2$ (15 mL) in a separatory funnel. The mixture of the solution formed two layers. The organic phase at the bottom was collected, and the aqueous phase at the top was supplemented with 15 mL of n-hexane. The collected organic phases obtained was added with excess anhydrous $Na_2SO_4$. The result were evaporated at a temperature below 60 °C. The product (EP) yielded a clear colorless liquid with a distinct aroma of fragrant ester compounds, which was calculated and analyzed using FT-IR and GC-MS.

### 2.4. Synthesis of 1,2-O-Isopropyliden Glycerol (IPG)

The IPG was synthesized by referring to previous study with modifying the materials used [14]. Glycerol (Gly) and acetone in a ratio of 1:2 were refluxed for 6 h at 80 °C under the control of thin-layer chromatography. The solution was added with 12.26 mmol $Na_2CO_3$ to neutralize. The mixture was extracted using n-hexane and distilled water as solvents. The collected organic phase was added with anhydrous $Na_2SO_4$. The results were evaporated at a temperature below 60 °C. The evaporation residue was purified again using distillation and vacuum pumps to obtain a pure IPG. The product studied was a colourless liquid, which was subjected to analysis using FT-IR and GC-MS.

### 2.5. Synthesis of IGA

The IGA compound was synthesized from EtOAc and IPG with a molar ratio of 1:8 through transesterification reaction, respectively. A mixture of 10 mmol EtOAc, 80 mmol IPG, and 5.47 mmol $Na_2CO_3$ was boiled at 140 °C for 30 h. The ethanol formed from this process was evaporated and added with distilled water to dissolve the excess IPG. The results were extracted using n-hexane with 3 repetitions. The accumulated organic phase was washed with distilled water, added with anhydrous sodium sulphate, and evaporated. The product of IGA was a clear, slightly yellowish liquid. The resulting IGA was calculated and analyzed using FT-IR, GC-MS, $^1$H-NMR, and $^{13}$C-NMR.

### 2.6. Synthesis of IGP

The IGP compound was synthesized from EP and IPG with a molar ratio of 1:8 through transesterification reaction, respectively. A mixture of 10 mmol EP, 80 mmol IPG, and 5.47 mmol $Na_2CO_3$ was refluxed at 140 °C for 30 h. The ethanol formed was evaporated and distilled water was added to dissolve the excess IPG. The result of the reaction was extracted with n-hexane with 3 repetitions. The collected organic phase was washed with distilled water, added with anhydrous sodium sulphate, and evaporated to remove the solvent. The product of IGP was a clear, slightly yellowish liquid. The products formed were calculated and analyzed with FT-IR, GC-MS, $^1$H-NMR, and $^{13}$C-NMR.

### 2.7. Antibacterial Test

The synthesized product, in the form of IGA and IGP respectively was dissolved in a 1% DMSO solvent with 5 different concentrations: 62.5, 125, 250, 500, and 1000 ppm. The antibiotic compound used as the positive control was amoxicillin at 100 ppm. DMSO solvent was used as the negative control test solution at a concentration of 1%. The preparation tools of antibacterial kit test were sterilized with absolute ethanol followed by an autoclave at a pressure of 15 psi and a temperature of 121 °C for 15 min.

The sterilized media was inoculated with *S. aureus* and *E. coli* bacteria at 37 °C. The resulting compounds were cultured and injected. The wells were made using a washer (6 mm diameter). Each well was injected with a negative control (DMSO 1%), a positive control (100 ppm amoxicillin), and the compound to be tested (IGA and IGP). The cultured test medium was left to solidify for 15 min on the media. The ring was taken and put into each well which was injected with the positive, negative, and test compound. This was incubated at 37 °C for 24 h, and the inhibition zone was measured using a vernier calliper. Compounds with a minimum inhibition zone of 16 mm were categorized as active compounds.

## 3. RESULT AND DISCUSSION

### 3.1. Synthesis of EP

The initial stage of this study involved the creation of ester compounds based on short-chain carboxylic acids, specifically ethyl propanoate (EP). PA is a carboxylic acid compound with a molecular weight of 74 g/mol and three carbon atoms. EP was synthesized using ethanol as both the reactant and solvent, along with PA using sulfuric acid as the catalyst. The mixture was reacted for 2 h at 80 °C using the Fischer esterification method. **Fig. 1** illustrates the formation of EP reaction equation.

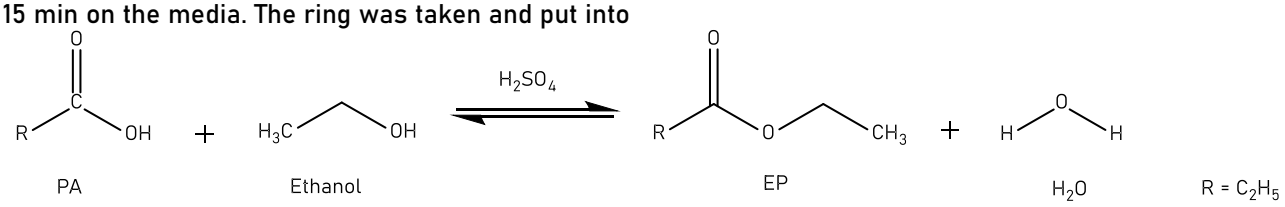


**Fig. 1**. Esterification reaction of PA to EP

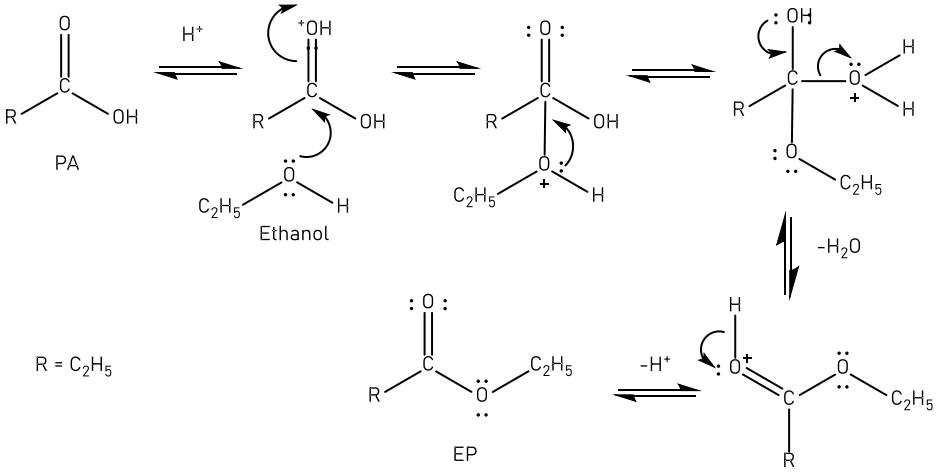


**Fig. 2** Mechanism of formation of EP esterification

The esterification reaction mechanism using an acid catalyst consist of several stages. The first is the protonation of the carbonyl group by $H^+$ ion from $H_2SO_4$ as the catalyst, followed by nucleophilic attack by ethanol, proton transfer from the $^+OHR_1$ ion to the -OH group, and the elimination of $H_2O$ molecules. This process resulted in the conjugate acid of the ester compound and released one proton to form the ester compound. For a more detailed explanation, refer to the esterification reaction mechanism shown in **Fig. 2**.

The EP obtained from the reaction of PA and ethanol with an $H_2SO_4$ catalyst was a clear liquid with a fragrant ester compound aroma and a yield of 37.72%. Furthermore, the EP was characterized using FT-IR and GC-MS. The results of the FT-IR analysis of the EP are presented in **Fig. 3a**. Several functional groups were detected, such as the carbonyl (C=O) ester group with strong absorption at 1744 $cm^{-1}$, supported by a weak absorption at 1196 $cm^{-1}$, indicating the carbonyl (C-O) ester group. The absorptions at 2986 and 2955 $cm^{-1}$ represented absorption peaks for $sp^3$ C-H groups. The carbonyl (C=O) group absorption in the range of 1735-1750 $cm^{-1}$ indicated characteristic wave number absorption for the formation of ester compounds. The results of the FT-IR spectrum analysis reveal that there

is an indication of the formation of the ester compound, namely EP.

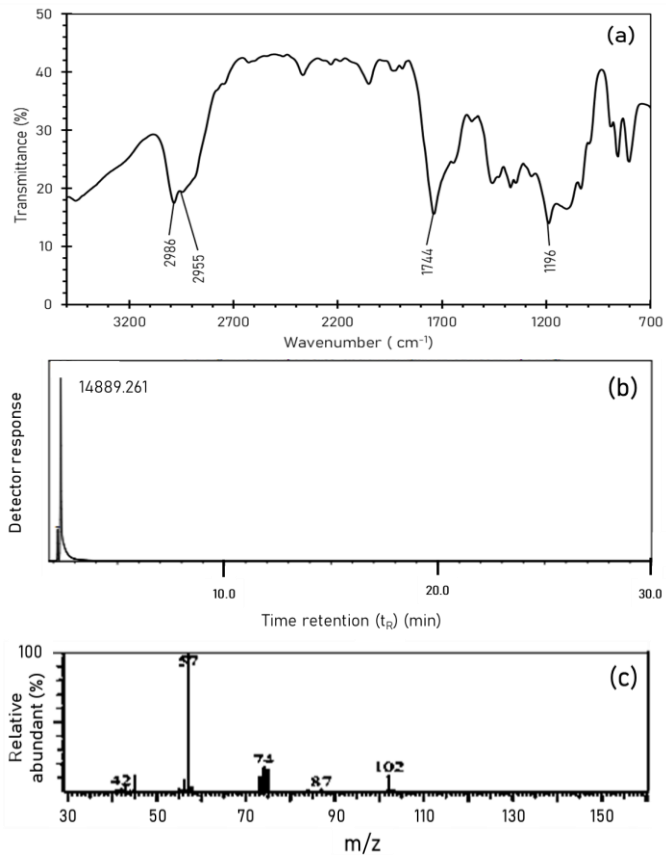


**Fig. 3** Infrared spectrum (a), chromatogram (b), and mass spectrum at $t_R$ = 2.34 min (c) of EP

Further analysis was conducted using GC-MS, resulting in the chromatogram presented in **Fig. 3b** and the mass spectra presented in **Fig. 3c**. Based on the GC chromatogram, there were two peaks, namely the first peak at a retention time ($t_R$) of 2.20 min and the second peak at a retention time ($t_R$) of 2.34 min. The second peak was predicted to be the EP target compound, with a relative purity of 91.66% and a yield of 37.72%.

The mass spectrum presented in **Fig. 3c** show the [$M^+$] molecular ion with m/z 102, which correspond to the molecular weight of EP, 102 g/mol. The molecular ion with m/z 102 experiences the loss of a methyl radical group, resulting in a fragment with m/z 87. This fragment subsequently loses the $CH_2O$ radical group, yielding the m/z 57 fragment (base peak). The molecular ions also undergone loss of the ethyl radical group, producing the m/z 74 fragment. The proposed fragmentation pattern of EP is presented in **Fig. 4**.

### 3.2. Synthesis of IPG

The IPG is a derivative of Gly that forms a cyclic compound due to the protection of two adjacent hydroxyl (-OH) groups on Gly. The protection of Gly is achieved through a condensation reaction with the derivative of ketone, namely acetone, forming a cyclic compound on its two hydroxyl groups. This reaction is referred to as the ketalization reaction [15].

The catalysis reaction was carried out through the reaction between Gly and acetone compounds using *p*TsOH as the catalyst and chloroform as the solvent. In the initial stage of the reaction, protonation of acetone will occur, causing the free electron pair on the oxygen atom of the hydroxyl group in glycerol to attack the electron-deficient carbon atom of the carbonyl group. Subsequently, a water molecule will be released, adding a positive charge to the oxygen atom. This will lead to the polarization of the C-O bond and the attack of other free electron pairs from the hydroxyl groups in glycerol on the carbon atom, forming a C-O bond and making it positively charged. In the final stage, a proton will be released, forming a ketal by bonding two hydroxyl groups in glycerol, resulting in IPG. The reaction mechanism for the IPG can be seen in **Fig. 5.**

The product of IPG produced through catalysis reaction was in the form of colorless liquid with a relatively 100% purity and a yield of 27.78%. The IPG compounds were further analyzed for their structure using FT-IR and GC-MS. The FT-IR spectrum analysis

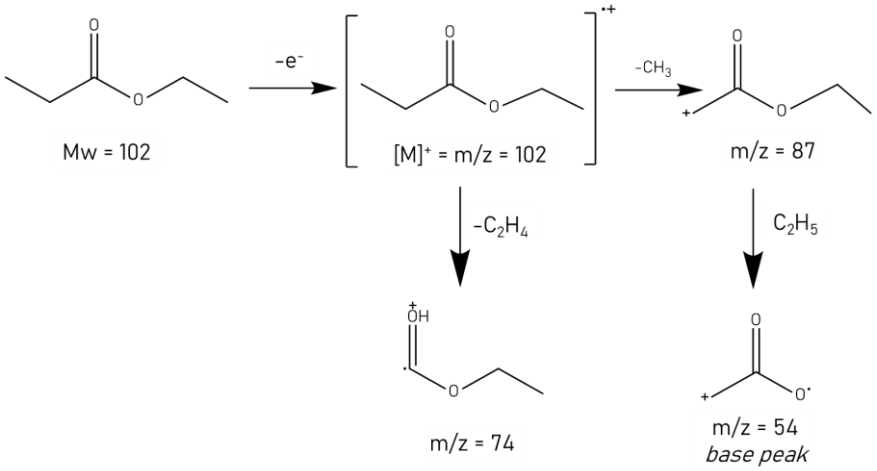


**Fig. 4** Fragmentation pattern of EP

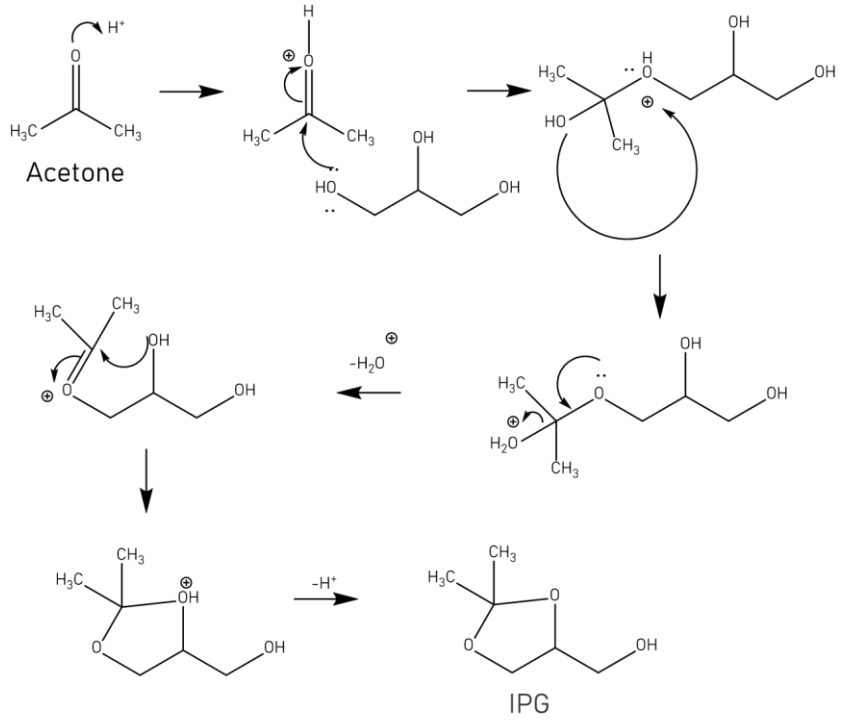


**Fig. 5.** Reaction mechanism for the formation of IPG

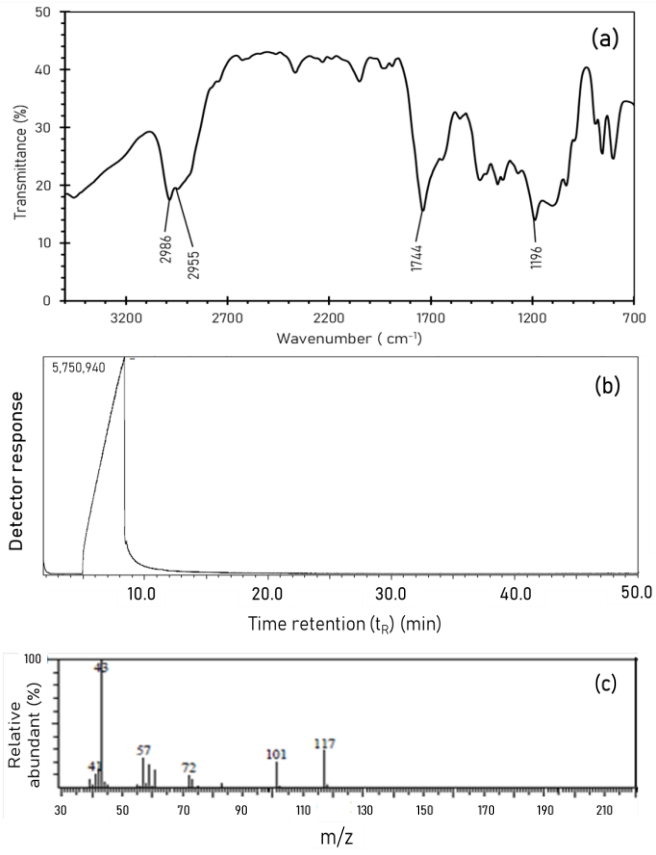


**Fig. 6** Infrared spectrum (a), chromatogram (b), and mass spectrum at $t_R$ = 8.34 min (c) of IPG

results for the IPG compounds was presented in **Fig. 6a**, showing the presence of absorption peaks in the wavenumber regions of 3418, 2994, and 1157 $cm^{-1}$ associated with specific functional groups. Additionally, absorption peaks for geminal methyl groups were also observed. The absorption peak at 2994 $cm^{-1}$ was assigned to the C-H stretch group. The FT-IR spectra indicate that IPG has been formed, as evidenced by the appearance of absorption peaks corresponding to the carbonyl (C=O) ester functional group at the wavenumber of 1157 $cm^{-1}$ and a strong absorption peak of the hydroxyl (OH) group at the wavenumber of 3418 $cm^{-1}$. This indicates the presence of hydroxyl (-OH) groups still bound to the IPG.

Further analysis of IPG was conducted using GC-MS, resulting in the GC chromatogram shown in **Fig. 6b** and its mass spectra in **Fig. 6c**. Based on the GC chromatogram, only one peak was observed at a retention time ($t_R$) of 8.34 minutes with a relative purity of 100%. The IPG product was successfully synthesized with a yield of 27.78%.

The presence of a single peak obtained was indicated as IPG. This is evidenced by its alignment with the fragmentation pattern of IPG with a molecular weight of 132 g/mol which has undergone successive fragmentation at m/z 117, 101, 72, 57, and 43 (base peak). The molecular ion peak ($M^+$) of IPG is not readable, but the appearance of fragmentation peaks at m/z 117 indicates homolytic cleavage with the loss of a methyl radical attached to the protected group.

The molecular ion fragment ($M^+$) underwent direct release of an alkyl group (methyl/-$CH_3$) attached to the cyclic IPG chain (**Fig. 6c**). The molecular ion also experiences the release of a radical methanol group, resulting in a fragment with m/z 101. Subsequently, the fragment pattern involves the release of a radical

aldehyde group, yielding a fragment with m/z 72. This fragment underwent heterogeneous cleavage at the methyl (-$CH_3$) group, producing a fragment with m/z 57. This fragment releases a –$CH_2$ group, resulting in a fragment with m/z 43, which is the base peak fragment or the fragment with the highest relative abundance. The m/z 43 fragment is stable because its positive

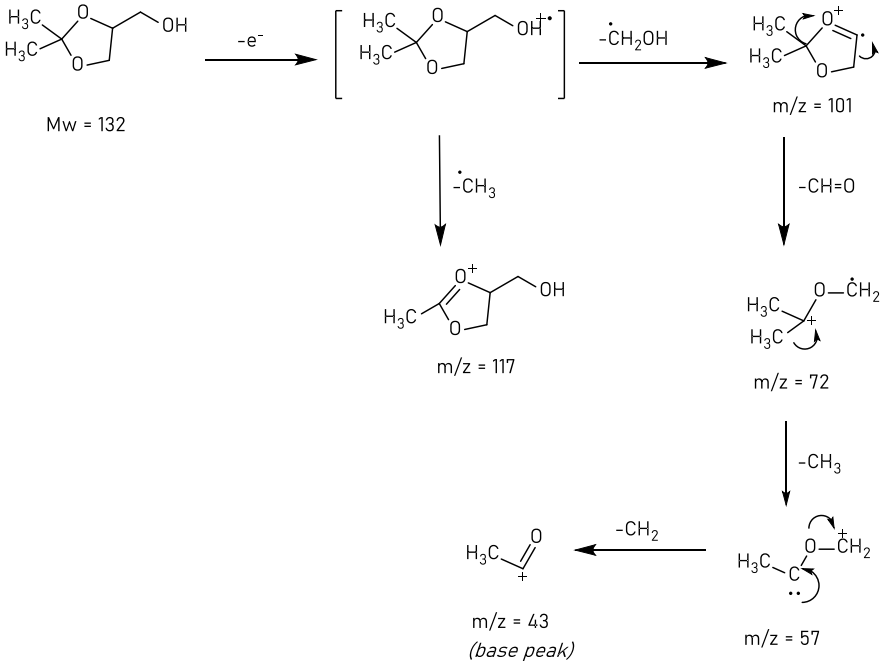


**Fig. 7** Fragmentation pattern of IPG

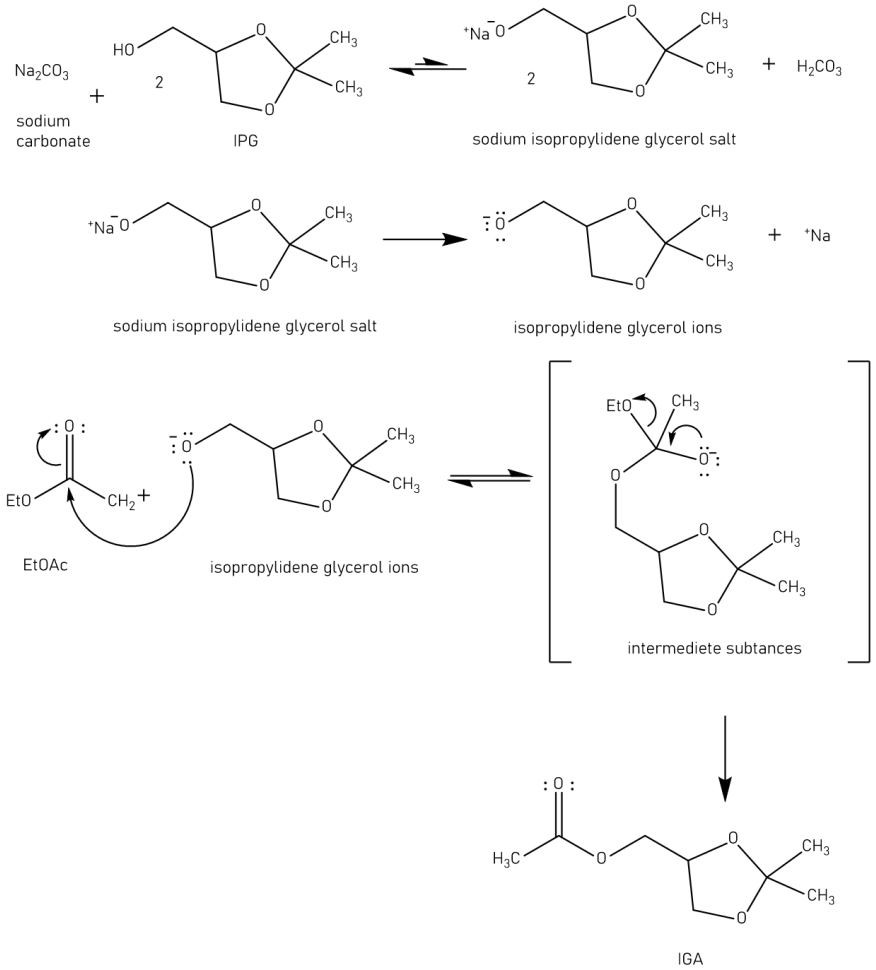


**Fig. 8.** The mechanism of transesterification reaction for the formation of IGA

charge can undergo delocalization. The proposed fragmentation pattern is presented in **Fig. 7**.

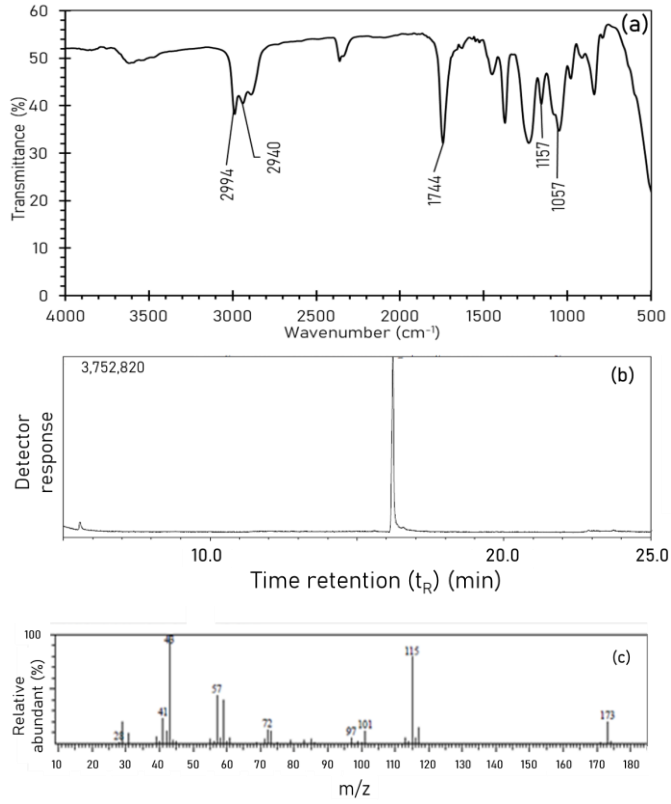


**Fig. 9** Infrared spectrum (a), chromatogram (b), and mass spectrum at $t_R$ = 16.22 min (c) of IGA

### 3.3. Synthesis of IGA

The IGA compound was obtained from the reaction between IPG and EtOAc using $Na_2CO_3$ as a catalyst. The transesterification reaction process for IGA formation is initiated with the attack of the base catalyst $Na_2CO_3$ on IPG, forming sodium isopropylidene glycerol salt. Subsequently, the sodium isopropylidene glycerol salt undergoes ionization into sodium ions and isopropylidene glycerol ions. The isopropylidene glycerol ion attackes the carbonyl carbon atom in EtOAc, forming an intermediate tetrahedral compound. The intermediate tetrahedral compound formed undergoes elimination, i.e., the cleavage of the acyl group, followed by the formation of the IGA compound and ethanolate ions. The mechanism of the transesterification reaction for IGA formation can be seen in **Fig. 8.**

The IGA product obtained was a clear, slightly yellowish liquid with a yield of 70.11%. The product was characterized for its structure using FT-IR, GC-MS, $^1$H-NMR, and $^{13}$C-NMR. The FT-IR analysis results for IGA is presented in **Fig. 9a**. It provides information about the appearance of several peaks, such as a very strong absorption peak at 1744 cm$^{-1}$ indicating the carbonyl (C=O) ester group and C-O ether group absorption at 1157 cm$^{-1}$. Absorption due to the C-O ether group was also observed at 1057 cm$^{-1}$. Absorption peaks at 2994 and 2940 cm$^{-1}$ corresponded to the C-H sp$^3$ group. Based on the FT-IR spectra, it was evidenced that IGA

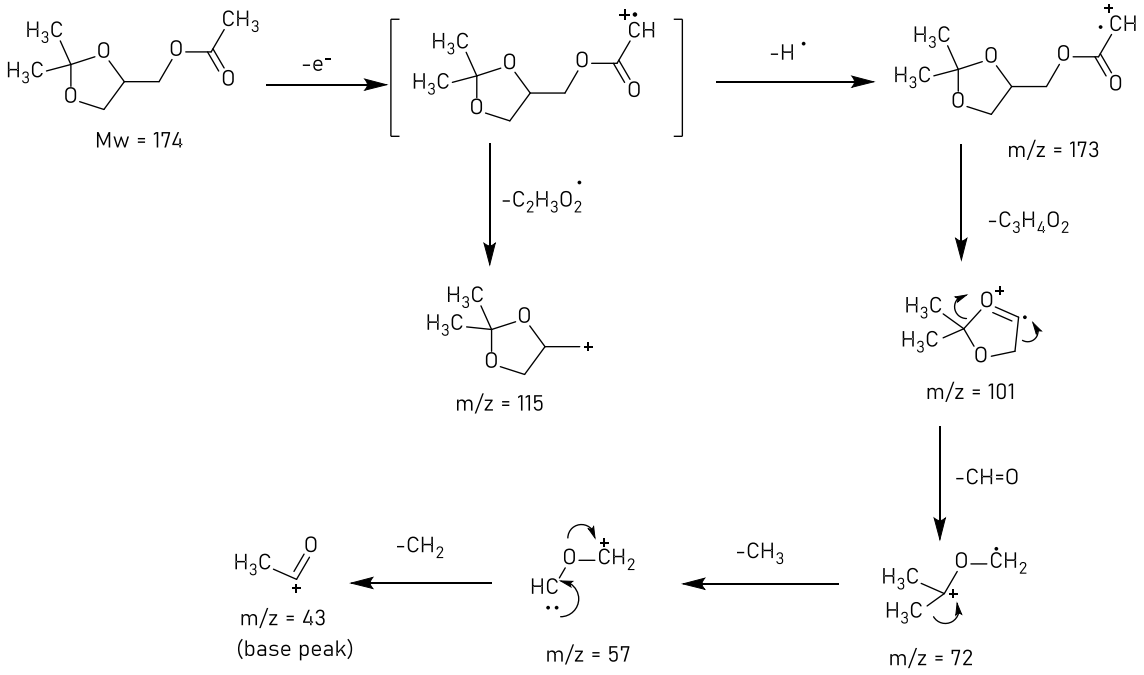


**Fig. 10** Fragmentation pattern of IGA

has been formed, particularly indicated by the distinctive absorption peak characteristic of ester compounds, which is very strong absorption in the 1750-1735 cm$^{-1}$ range for the carbonyl (C=O) ester group. Absorption due to the hydroxyl (-OH) group was not observed in the 3700-3300 cm$^{-1}$ region. This finding indicates that the hydroxyl groups of IPG have been substituted by groups from an ester compound.

Further elucidation of the IGA structure was conducted using GC-MS, resulting in the GC chromatogram shown in **Fig. 9b** and the mass spectra in **Fig. 9c**. The GC chromatogram showed only one peak at a retention time ($t_R$) of 16.22 min with a relative purity of 100%. It is confirmed by the consistent fragmentation pattern of the molecular ion ($M^+$) of IGA after the release of one hydrogen atom radical (H·), resulting in a fragment with m/z 173. IGA has a molecular weight of 174 g/mol, but in the interpretation of the detected mass spectra, the first detected ion is not the molecular ion ($M^+$).

**Fig. 9c** show that the detected molecular ion ($M^+$) was at m/z 173, indicating that the IGA has undergone the release of one hydrogen radical atom. Furthermore, the fragment at m/z 173 releases a $C_2H_2O_2$ radical to generate the fragment at m/z 115. The molecular ion ($M^+$) also experiences the release of a $C_6H_{12}O_3$ radical, producing the fragment at m/z 43 (base peak). The molecular ion ($M^+$) detected at m/z 173 also underwent successive fragmentation with the release of $C_5H_9O_2$ and $CH_2$ radicals, resulting in fragments at m/z 72 and m/z 57, respectively. The proposed fragmentation pattern is displayed in **Fig. 10**.

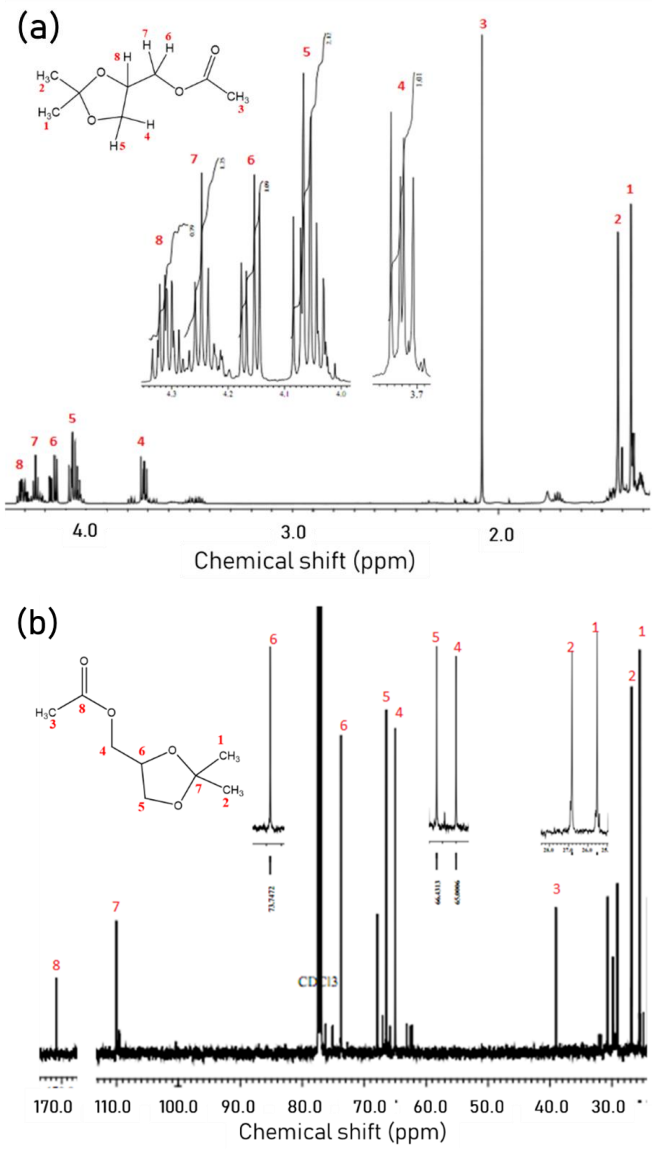


**Fig. 11** $^1$H-NMR spectrum (a) and $^{13}$C-NMR spectrum (b) of IGA

The IGA was also analyzed using $^1$H-NMR and $^{13}$C-NMR to reinforce its structure. The $^1$H-NMR spectra of IGA in **Fig. 11a** show the presence of 8 non-equivalent proton peaks. The integration values indicate a total of 14 protons, consistent with the proton count in the IGA compound. The $^1$H-NMR spectra reveal distinct chemical shift appearances. The proton peak 1 (δ 1.36 ppm) and proton 2 (δ 1.42 ppm) exhibited singlet appearances with an integration of 3, corresponding to the protons of the methyl (-$CH_3$) group attached to geminal carbon atoms. Proton 3, with a chemical shift of δ 2.08 ppm and a singlet appearance, represented the methyl (-$CH_3$) group attached to an oxygen atom (ester group). Peaks 4, 5, 6, and 7, with chemical shifts at 3.74, 4.07, 4.17, and 4.26 ppm respectively, displayed doublet of doublet appearances. Protons 4, 5, 6, and 7 were coupled to proton 8, resulting in the doublet appearance. Additionally, protons 4 and 5 coupled with each other, generating the doublet of doublet appearance. The doublet of doublet (dd) peak consisted of four lines resulting from two protons (or other spin ½ nuclei), and the lines had equal intensities (or closely equal intensities). Protons 4, 5, 6, and 7 were located in the -$CH_2$- group neighbouring the chiral carbon atom, making the protons in the -$CH_2$- group diastereotopic.

Based on the analysis of $^1$H-NMR results of IGA, it was shown by the presence of peaks 1 and 2, which were geminal methyl groups exhibiting chemical shifts δ 1.36 and δ 1.42 ppm from the –$CCH_3CH_3$ proton with a singlet signal appearance. The proton peak on the carbon atom of the geminal methyl group (-$CH_3$) was also visible at a chemical shift of δ 1.36 ppm with a singlet signal appearance in the synthesis of IGA with a purity of 99% and a yield of 97% [14]. The peak shift patterns of 1 and 2 are located in the upfield or shielded region because geminal methyl groups were not bonded to electronegative atoms. The singlet signal appearance on peaks 1 and 2 indicates that the protons on the methyl groups (-$CCH_3$) are not coupled because there are no protons on neighbouring carbon atoms. This suggests the possibility of a cyclic reaction leading to the formation of IGA and the presence of a proton from the chiral centre formed in the cyclic chain. Furthermore, the absorption of proton peaks at a shift of δ 4.32 ppm with a multiplet signal appearance indicates the presence of protons on the chiral centre atom [14].

The identification of IGA structure was further carried out using $^{13}$C-NMR, as shown in **Fig. 11b**. The presence of 8 non-equivalent peaks. The $^{13}$C-NMR spectrum results indicates 8 carbon atom peaks in distinct environments. The number of carbon atoms corresponded to the carbon atom count in the IGA. The carbon atoms of IGA observed in the $^{13}$C-NMR spectrum exhibited chemical

shifts at 25.7, 26.9, 30.9, 65, 66.4, 73.64, 110.9, and 170.2 ppm. Peaks 1 and 2, located in the upfield region with chemical shifts at δ 25.7 and δ 26.9 ppm, were absorptions from two geminal methyl (-$CH_3$) groups. These two geminal methyl groups are in the upfield region due to being only attached to a single carbon atom and are far from the oxygen atoms in the electronegative cyclic chain. The presence of peak 3 at a different chemical shift region, δ 30.9 ppm, is presumed to be the absorption of a $Csp^3$ carbon atom bonded to a methyl group (-$OCH_3$).

Based on the results of the $^{13}$C-NMR spectrum analysis, the synthesized compound is suspected to be IGA. This can be observed from the appearance of peak 3, which corresponds to the carbon atoms in the methyl group (-$CH_3$), with a chemical shift at δ 30.9 ppm, and peak 8, which represents carbon atoms in the carbonyl group (C=O), with a chemical shift at δ 170.4 ppm. This is in accordance with the characteristic absorptions of IGA, which have a chemical shift for carbon atoms in the carbonyl (C=O) ester group at δ 150 – 170 ppm. Peak 3, corresponding to carbon atoms in the methyl group (-$OCH_3$) with a shift at δ 30.9 ppm, bound to the oxygen groups of the carbonyl ester compound, which had a high electronegativity, causing electrons to be strongly attracted towards oxygen, resulting in the signal being in an unprotected region. Therefore, the structural analysis using FT-IR, GC-MS, $^1$H-NMR, and $^{13}$C-NMR led to the conclusion that the formed compound was IGA, with a purity of 100% according to GC-MS and a yield of 70.11%.

### 3.4. Synthesis of IGP

The IGP was obtained from the reaction between IPG and EP using $Na_2CO_3$ as a catalyst. The transesterification reaction process in synthesizing IGP followed the same method as the synthesis of IGA. The transesterification reaction mechanism for IGP formation can be observed in **Fig. 12**. The IGP was in the form of a slightly yellowish clear liquid with a yield of 63.83%.

The product of IGP was characterized using FT-IR, GC-MS, $^1$H-NMR, and $^{13}$C-NMR. The FT-IR analysis results for IGP are presented in **Fig. 13a**. Some functional groups present were carbonyl (C=O) ester group appearing at the wavenumber of 1744 $cm^{-1}$, carbonyl (C-O) ether group at wavenumbers 1157 and 1057 $cm^{-1}$, and absorption at wavenumber 1219 $cm^{-1}$ due to the carbonyl (C-O) ester group. The IGP has been

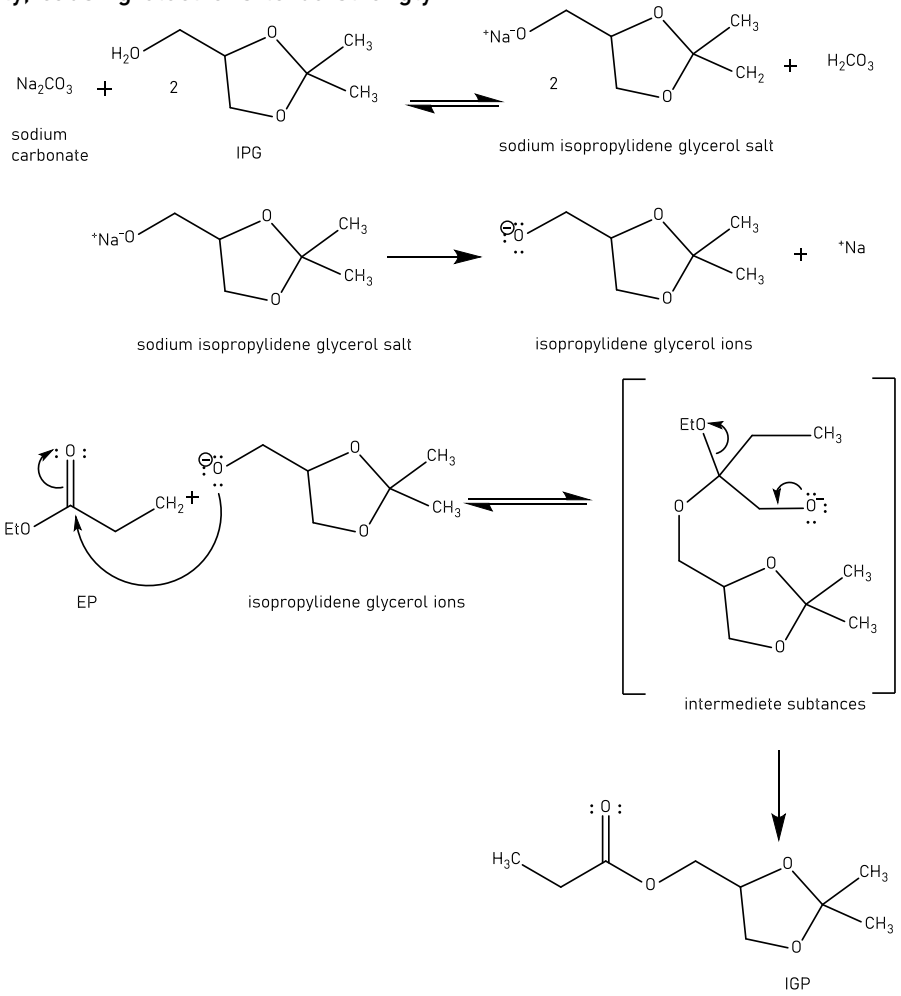


**Fig. 12**. The mechanism of transesterification reaction for the formation of IGP

to the carbonyl (C-O) ester group. The IGP has been proven to have formed based on FT-IR spectra, particularly the characteristic absorption peaks of ester compounds, which show a very strong absorption band for the carbonyl (C=O) group of ester at the absorption wave numbers of 1750-1735 $cm^{-1}$. Furthermore, the absence of absorption bands for the hydroxyl (-OH) group in the wave number range of

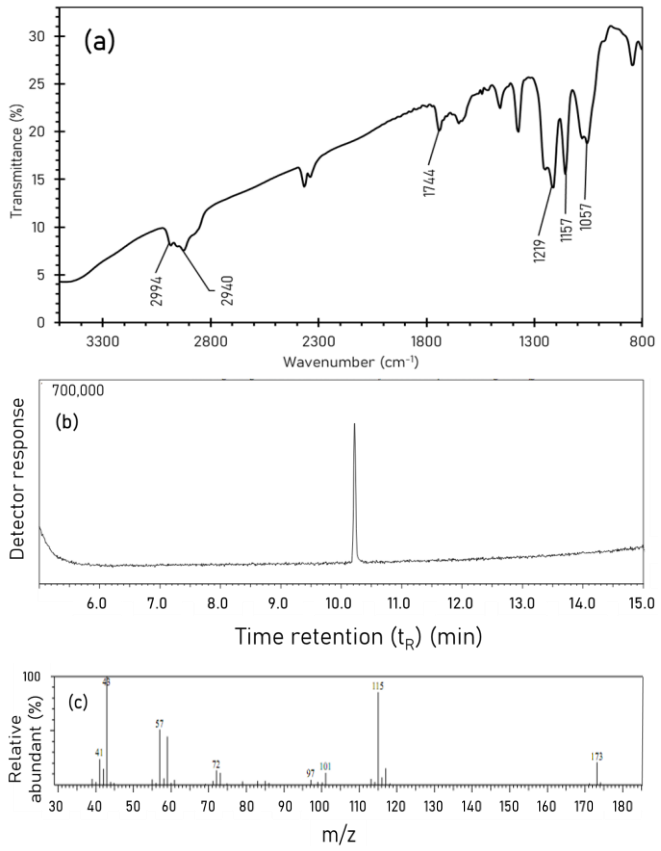


**Fig. 13** Infrared spectrum (a), chromatogram (b), and mass spectrum at $t_R$ = 10.22 min (c) of IGP

3500-3300 $cm^{-1}$ indicates that the hydroxyl groups of IPG have been substituted by groups from the ester compound.

Further analysis of the IGP was conducted using GC-MS, which produced a GC chromatogram as shown in **Fig. 13b** and its mass spectra in **Fig. 13c**. The GC chromatogram showed a single peak at a retention time ($t_R$) of 10.22 min with a relative purity of 100% and a yield of 63.83%.

The appearance of a single peak in the chromatogram was indicated as IGP. This is confirmed by the matching fragmentation pattern of the molecular ion ($M^+$) of IGP, which was 173. This compound has a molecular weight of 188 g/mol, so in the interpretation of the mass spectra, the observed pattern is the fragment pattern after the release of an alkyl group, namely a methyl group (-$CH_3$). Based on the mass spectra in **Fig. 13c**, the detected molecular ion ($M^+$) had a m/z 173. This indicates the loss of a methyl (-$CH_3$) group from the intact gas-phase ion. This fragment also released a radical $C_2H_2O_2$, resulting in a fragment at m/z 115. The molecular ion ($M^+$) also undergone the loss of a radical $C_6H_{12}O_3$, generating a fragment at m/z 43 (base peak). The molecular ion ($M^+$) with m/z 173 further underwent the loss of a radicals $C_5H_9O_2$ and $CH_2$, producing fragments at m/z 72 and m/z 57, respectively. The proposed fragmentation pattern is shown in **Fig. 14**.

The IGP compound formed from the transesterification synthesis reaction was further analyzed using $^1$H-NMR and $^{13}$C-NMR to support its structure. The $^1$H-NMR spectra of IGP are presented in **Fig. 15a**, showing the presence of 9 non-equivalent proton peaks. The appearance of a triplet signal with an integration of 3 at a chemical shift δ of 1.13 ppm, corresponded to the peak of methyl (-$CH_3$) protons on -$CH_2$COOR. The observed peak 4 at a chemical shift δ of 2.36 ppm with a quartet appearance and an integration of 2 represented the -$CH_2$- group directly bound to the carbonyl (C=O) ester carbon. The absorption of 9 proton peaks at a shift of δ 4.23 ppm with a multiplet appearance and an integration of 1 indicated proton on the chiral central carbon atom.

The identification of the structure of IGP was continued using $^{13}$C-NMR (**Fig. 15b**). The presence of 9 non-equivalent peaks in the same environment. The number of carbon atoms corresponded to the number of carbon atoms in the IGP. The carbon atom peaks of the IGP were displayed in the $^{13}$C-NMR spectra with chemical shifts at δ 14.26, 25.58, 26.85, 29.83, 64.74, 67.04, 75.1, 109.9, and 174.39 ppm. Based on the results of the $^{13}$C-NMR spectral analysis, the synthesized compound was suspected to be IGP. This can be observed by the appearance of peak 1, which corresponds to the carbon atoms in the methyl (-$CH_3$) group, with a chemical shift at δ 14.26 ppm. Additionally, peak 4, representing the -$CH_2$- carbon atom bound to the carbonyl (C=O) ester group, appeares at a chemical shift of δ 29.83 ppm.

Furthermore, the peak of the carbon atoms at a shift of δ 29.7 ppm, corresponding to the -$CH_2$- carbon atoms in the downfield region, is due to the electron-withdrawing effect from the carbonyl (C=O) ester group. This effect is also evident in the synthesis of isopropylidene glycerol stearate [14]. Moreover, the appearance of a peak at a chemical shift of δ 14.1 ppm, corresponding to the carbon atoms in the methyl group (-$(CH_2)_{16}CH_3$) at the terminal part and in the upfield region, is due to the location of the methyl groups far from or unbound to electronegative atoms [14]. Peak 9, located in the farthest downfield region with a chemical shift of δ 174.39 ppm, represented the carbon atom in the carbonyl (C=O) ester group, which had high electronegativity. This causes strong electron attraction towards oxygen and places the peak signal in an unprotected region. Therefore, it can be concluded that the synthesized compound was IGP with a purity of 100% and a yield of 63.83%.

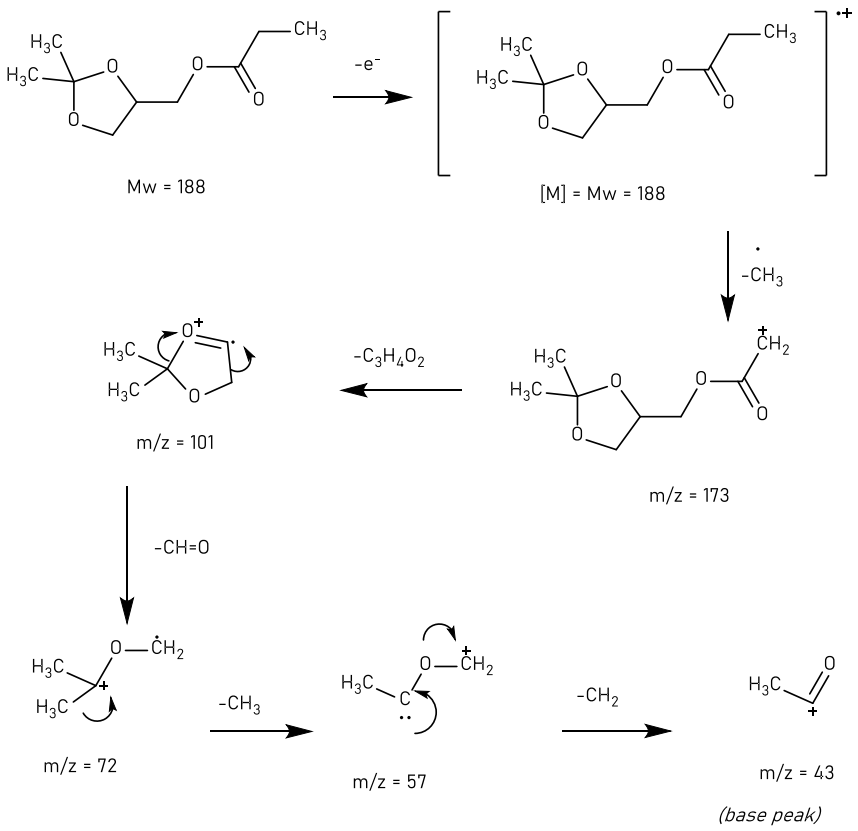


**Fig. 14**. Fragmentation pattern of IGP

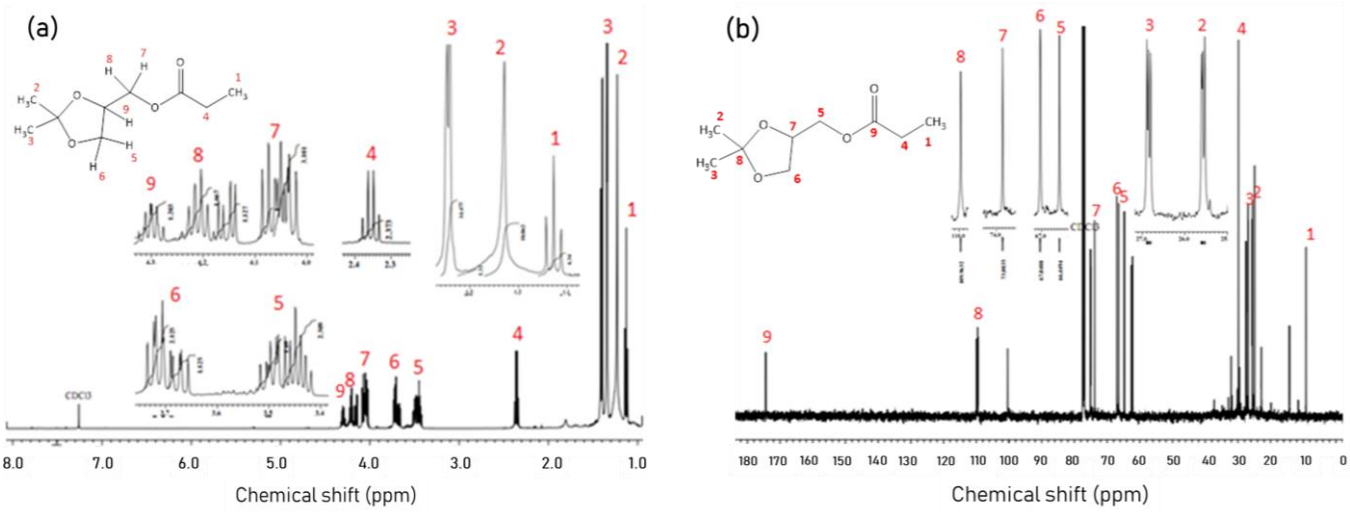


**Fig. 15** $^{1}$H-NMR spectrum (a) and $^{13}$C-NMR spectrum (b) of IGP

### 3.5. Antibacterial Test

The results of the antibacterial activity potential observation against IGA and IGP compounds are presented in **Table 1**. Neither IGA nor IGP compounds had any inhibitory effects on the growth of bacteria, including Gram-negative bacteria *E. coli* and Gram-positive bacteria *S. aureus*. The test compounds failed to exhibit any growth-inhibiting activity against bacterial cells, even when tested at the maximum concentration of 1000 ppm. The lack of antibacterial activity in both test compounds is likely due to the cyclic structure of IGA and IGP, which does not contain hydroxyl groups as part of the hydrophilic moiety. The absence of hydrophilic groups (-OH groups) in IGA and IGP compounds make it difficult for these compounds to interact with the membranes of the test bacterial cells.

The results of the synthesis and activity testing of IGA and IGP that did not possess inhibitory activity against bacterial cell growth necessitate further reactions involving deprotection of glycerol in its cyclic compound form. This is done to expose the protected groups and formed monoglyceride compounds, monoacetin and monopropionin, each containing two hydroxyl (-OH)

groups that function as hydrophobic groups. Another factor in IGA and IGP compounds lacking inhibitory capabilities against bacterial cell growth may be attributed to the active carbon chain in their hydrophobic regions, which are synthesized from short-chain carboxylic acid esters, resulting in smaller molecular sizes compared to other monoglyceride derivatives such as monolaurin, monostearin, and monoolein formed from medium or long-chain carboxylic acid esters.

**Table 1**. The results of the antibacterial activity potential against IGA and IGP

| Compounds | Diameter of inhibition zone in bacteria (cm) | |
|---|---|---|
| | *S. aureus* | *E. coli* |
| IGA 62.5 ppm | - | - |
| IGA 125 ppm | - | - |
| IGA 250 ppm | - | - |
| IGA 500 ppm | - | - |
| IGA 1000 ppm | - | - |
| IGP 62.5 ppm | - | - |
| IGP 125 ppm | - | - |
| IGP 250 ppm | - | - |
| IGP 500 ppm | - | - |
| IGP 1000 ppm | - | - |
| Positive control (amoxicillin 100 ppm) | 4.45 | 2.85 |
| Negative control (DMSO 1%) | - | - |

## CONCLUSION

The synthesis of the ester compound in the form of EP through esterification reaction with 98% sulfuric acid catalyst yielded a relative purity of 91.66% and a yield of 37.72%. Additionally, the IPG was obtained by glycerol protection, resulting in a relative purity of 100% based on GC-MS analysis and a yield of 27.78%. The transesterification reaction between EtOAc and EP with IPG formed IGA and IGP with a relative purity of 100% based on GC-MS analysis, and their respective yields were 70.11% and 63.83%. At concentrations of 62.5, 125, 250, 500, and 1000 ppm, neither IGA nor IGP compounds might prevent the growth of gram-positive bacteria *S. aureus* nor gram-negative bacteria *E. coli*.

## SUPPORTING INFORMATION

There is no supporting information of this paper. The data that support the findings of this study are available on request from the corresponding author (AR).

## ACKNOWLEDGEMENTS

AR and LC would like to extend their gratitude to the Pharmacy Vocational Program as well as the Pharmacy and Food Analysis Vocational Program at the Politeknik Kesehatan Kemenkes Surakarta Kampus III Klaten for all of the support they received while working on this manuscript. The authors would also like to express their gratitude to CV. ARD Pratama for their assistance in providing the necessary equipment and chemical ingredients for this study.

## CONFLICT OF INTEREST

All authors declare that there is no conflict of interest.

## AUTHOR CONTRIBUTIONS

AR, LC, and FR conducted the experiment and interpreted the laboratory data. AR, FR, BI, and AI wrote the manuscript. AR, BI, and AI revised the manuscript. All authors agreed to the final version of this manuscript.

## REFERENCES

[1] Pegu, K., More, P., & Arya, S.S. 2023. Application of different orifices for hydrodynamic cavitational effects on deactivation of Escherichia coli and Staphylococcus aureus in milk. *Food Bioprod. Process.* 141. 49–59. doi: 10.1016/j.fbp.2023.07.003.

[2] Afzali, S., Doosti, A., Heidari, M., Babaei, N., Keshavarz, P., Nadem, Z., & Kahnamoei, A. 2021. Effects of Staphylococcus aureus enterotoxin type A on inducing the apoptosis in cervical cancer cell line. *Gene Reports*. 25. 101397. doi: 10.1016/j.genrep.2021.101397.

[3] He, Q., Liu, D., Ashokkumar, M., Ye, X., Jin, T.Z., & Guo, M. 2021. Antibacterial mechanism of ultrasound against Escherichia coli: Alterations in membrane microstructures and properties. *Ultrason. Sonochem.* 73. 105509. doi: 10.1016/j.ultsonch.2021.105509.

[4] Nirmal, N.P., Chunhavacharatorn, P., Chandra Khanashyam, A., Li, L., & Al-Asmari, F. 2023. Cinnamon bark oil in water nanoemulsion formulation, characterization, and antimicrobial activities. *LWT*. 179(4). 114671. doi: 10.1016/j.lwt.2023.114671.

[5] Yang, D., Jiang, Z., Meng, Q., Wang, S., Pan, H., Rao, L., & Liao, X. 2023. Analyzing the pressure resistant, sublethal injury and resuscitable viable but non-culturable state population of Escherichia coli, Staphylococcus aureus, Bacillus amyloliquefaciens and Lactiplantibacillus plantarum under high pressure processing. *Food Res. Int.* 173(P1). 113336. doi: 10.1016/j.foodres.2023.113336.

[6] Yuann, J.M.P., Lee, S.Y., He, S., Wong, T.W., Yang, M.J., Cheng, C.W., Huang, S.T., & Liang, J.Y. 2022. Effects of free radicals from doxycycline hyclate and minocycline hydrochloride under blue light irradiation on the deactivation of Staphylococcus aureus, including a methicillin-resistant strain. *J. Photochem. Photobiol. B. Biol.* 226. 112370. doi: 10.1016/j.jphotobiol.2021.112370.

[7] Guan, G., Zhang, L., Zhu, J., Wu, H., Li, W., & Sun, Q. 2021. Antibacterial properties and mechanism of biopolymer-based films functionalized by CuO/ZnO nanoparticles against

Escherichia coli and Staphylococcus aureus. *J. Hazard. Mater.* 402. 123542. doi: 10.1016/j.jhazmat.2020.123542.

[8] Roy, A.S., Cheruvathoor Poulose, A., Bakandritsos, A., Varma, R.S., & Otyepka, M. 2021. 2D graphene derivatives as heterogeneous catalysts to produce biofuels via esterification and trans-esterification reactions. *Appl. Mater. Today*. 23. 101053. doi: 10.1016/j.apmt.2021.101053.

[9] Kim, J., Yu, H., Yang, E., Choi, Y., & Chang, P.S. 2023. Effects of alkyl chain length on the interfacial, antibacterial, and antioxidative properties of erythorbyl fatty acid esters. *LWT*. 174. 114421. doi: 10.1016/j.lwt.2022.114421.

[10] Moussaoui, O. *et al.* 2021. Selective synthesis of novel quinolones-amino esters as potential antibacterial and antifungal agents: Experimental, mechanistic study, docking and molecular dynamic simulations. *J. Mol. Struct.* 1241. 130651. doi: 10.1016/j.molstruc.2021.130652.

[11] Patel, N.K. & Shah, S.N. 2015. *Biodiesel from Plant Oils*. Elsevier Inc. doi: 10.1016/B978-0-12-800211-7.00011-9.

[12] Park, S.H. & Kim, H.K. 2020. Antibacterial activity of emulsions containing unsaturated fatty acid ergosterol esters synthesized by lipase-mediated transesterification. *Enzyme Microb. Technol.* 139. 109581. doi: 10.1016/j.enzmictec.2020.109581.

[13] Natalia, A., Kim, S. jin, & Kim, H.K. 2016. Antioxidant and antibacterial activity of fatty acid vanillyl ester produced by Proteus vulgaris K80 lipase-mediated transesterification. *J. Mol. Catal. B Enzym.* 133. S475–S481. doi: 10.1016/j.molcatb.2017.03.012.

[14] Yu, C.C., Lee, Y.S., Cheon, B.S., & Lee, S.H. 2003. Synthesis of Glycerol Monostearate with High Purity. *Bull. Korean Chem. Soc.* 24(8). 1229–1231. doi: 10.5012/bkcs.2003.24.8.1229.

[15] [15] Gao, S., Liang, X., Wang, W., Cheng, W., & Yang, J. 2007. High efficient acetalization of carbonyl compounds with diols catalyzed by novel carbon-based solid strong acid catalyst. *Chinese Sci. Bull.* 52(21). 2892–2895. doi: 10.1007/s11434-007-0363-1.